# The Ionoregulatory Responses to Hypoxia in the Freshwater Rainbow Trout *Oncorhynchus mykiss*

**Fathima I. Iftikar**[1,*]
**Victoria Matey**[2,†]
**Chris M. Wood**[1,‡]
[1]Department of Biology, McMaster University, Hamilton, Ontario L8S 4K1, Canada; [2]Department of Biology, San Diego State University, 5500 Campanile Drive, San Diego, California 92182

Accepted 9/27/2009; Electronically Published 1/22/2010

## ABSTRACT

We utilized the rainbow trout, a hypoxia-intolerant freshwater teleost, to examine ionoregulatory changes at the gills during hypoxia. Progressive mild hypoxia led first to a significant elevation (by 21%) in $J^{Na}_{influx}$ (measured with $^{22}Na$), but at 4-h hypoxia when $Po_2$ reached ~110 mmHg, there was a 79% depression in $J^{Na}_{influx}$. Influx remained depressed during the first hour of normoxic recovery but was restored back to control rates thereafter; there were no significant changes in $J^{Na}_{efflux}$ or $J^{Na}_{net}$. A more prolonged (8 h) and severe hypoxic (~80 mmHg) exposure induced a triphasic response whereby $J^{Na}_{influx}$ was significantly elevated during the first hour, as during mild hypoxia, but returned to control rates during the subsequent 3 h. Thereafter, rates started to gradually increase and remained significantly elevated by about 38% through to 8 h of hypoxia. A similar triphasic trend was observed with $J^{Na}_{efflux}$ but with larger changes than in $J^{Na}_{influx}$, such that negative $Na^+$ balance occurred during the hypoxic exposure. Net $K^+$ loss rates to the water approximately doubled. There were no significant alterations in ammonia excretion rates in either of the hypoxia regimes. Branchial $Na^+/K^+$-ATPase activity did not change during 4 h at $Po_2 \sim 80$ mmHg or return to normoxia; $H^+$-ATPase activity also did not change during hypoxia but was significantly depressed by ~75% after 6 h of normoxic recovery. Scanning electron microscopy revealed that within 1 h of exposure to $Po_2 \sim 80$ mmHg, exposed mitochondria-rich cell (MRC) numbers increased by 30%, while individual MRC exposed surface area and total MRC surface area both increased by three- to fourfold. MRC numbers had decreased below control levels by 4 h of hypoxia, but surface exposure remained elevated by approximately twofold, a response that persisted through 6 h of normoxic recovery. Environmental hypoxia induces complex changes in gill ionoregulatory function in this hypoxia-intolerant species that are very different from those recently reported in the hypoxia-tolerant Amazonian oscar.

## Introduction

Aquatic hypoxia is increasing globally mainly as a result of anthropogenic inputs of nutrients (Diaz et al. 2004). During hypoxia, the demands to maintain ion regulation may conflict with the requirements for gas exchange, because freshwater fish are continuously faced with the problem of water influx and ion loss at the gills (Evans et al. 2005; Marshall and Grosell 2006). Specifically, an increase in functional branchial surface area to promote oxygen uptake under hypoxia would be expected to accelerate the loss of ions to the surrounding water, while reductions of surface area to lower ion loss may reduce the ability of the gill to take up oxygen (the osmorespiratory compromise; Randall et al. 1972; Nilsson 1986). In addition, environmental hypoxia may result in oxygen starvation of ATP-dependent transport processes.

Until recently, there has been little investigation of how hypoxia affects ionoregulation in freshwater fish. A slight stimulation of net branchial $Na^+$ and $Cl^-$ losses under hypoxia has been measured in one previous study on the hypoxia-intolerant rainbow trout, but results were confounded by fecal contamination of the water (Thomas et al. 1986). However a recent series of studies on the very hypoxia-tolerant Amazonian oscar, *Astronotus ocellatus*, has rekindled interest in this area (Richards et al. 2007; Wood et al. 2007, 2009; Scott et al. 2008). The oscar exhibits a rapid, profound reduction of both unidirectional $Na^+$ uptake and unidirectional $Na^+$ efflux during acute severe hypoxia, so that net $Na^+$ flux is not altered. Branchial $Na^+/K^+$-ATPase activity, ammonia and urea excretion, $K^+$ loss rates, and water exchange rates are also reduced, and the apical crypts of mitochondria-rich cells (MRCs) are largely covered over by pavement cells, suggesting that a general reduction in gill permeability occurs (Wood et al. 2007, 2009). This would appear to be an adaptive strategy to maintain ionoregulatory status in the face of unavoidable oxygen deprivation, because in the Amazon, oscars often cannot escape hypoxic conditions in their natural environment. Consequently, they possess the capacity to downregulate aerobic metabolism (Muusze et al. 1998; Sloman et al. 2006; Scott et al. 2008) and upregulate glycolysis

* Corresponding author. Present address: School of Biological Sciences, University of Auckland, Private Bag 92019, Auckland 1142, New Zealand; e-mail: iftikafi@gmail.com.
† E-mail: kuperman@sunstroke.sdsu.edu.
‡ E-mail: woodcm@univmail.cis.mcmaster.ca.

*Physiological and Biochemical Zoology* 83(2):343–355. 2010.  1522-2152/2010/8302-8202$15.00
DOI: 10.1086/648566

(Almeida-Val et al. 2000; Richards et al. 2007; Scott et al. 2008) so as to survive hypoxia.

In this study, we examined changes in branchial unidirectional and net $Na^+$ fluxes, net ammonia flux, $Na^+/K^+$-ATPase and $H^+$-ATPase activities, and gill surface morphology (by SEM) during several hypoxia regimes in the hypoxia-intolerant rainbow trout for comparison with those of the hypoxia-tolerant oscar. Complex alterations in branchial blood perfusion (Holeton and Randall 1967*a*; Booth 1979; Soivio and Tuurala 1981; Sundin and Nilsson 1997), increased branchial water flow (Holeton and Randall 1967*b*), and increased gill $O_2$ transfer factor (Randall et al. 1967) have all been observed in trout subjected to hypoxia and might be expected to increase branchial ion losses. Therefore, our first hypothesis was that unidirectional $Na^+$ efflux rates to the water should increase in trout under hypoxia. Because trout generally increase ammonia production and efflux rates at times of stress (Wood 2001), our second hypothesis was that ammonia excretion would not be decreased during hypoxia, in contrast to the oscar. Our third hypothesis was that a reduction in $Na^+$ influx rates from the water would occur during hypoxia either as a cost-saving measure or as a consequence of $O_2$ starvation of the ionocytes. Our fourth hypothesis was that associated reductions in $Na^+/K^+$-ATPase and $H^+$-ATPase activities (as measured by in vitro capacity under optimal conditions) would also likely occur; notably, the former decreased markedly in the oscar after 3–4 h of hypoxia (Richards et al. 2007; Wood et al. 2007). Two key indicators of severe oxygen deprivation are a rapid depletion of cellular ATP and a resultant loss of intracellular $K^+$ as the $Na^+/K^+$ pump begins to fail (Boutilier and St-Pierre 2000). Therefore, our fifth hypothesis was that $K^+$ leakage rates to the water, which are thought to occur largely via the transcellular route in trout gills (Lauren and McDonald 1985), would increase during hypoxia. Wood et al. (2009) reported that rates of branchial $K^+$ loss fell in oscar during hypoxia whereas paracellular permeability remained unchanged, supporting the idea that $K^+$ flux is largely a transcellular phenomenon. Our final hypothesis was that if gill morphological alterations occurred at all in the hypoxia-intolerant rainbow trout, they would be far less marked than the dramatic changes associated with permeability reduction in the oscar (Wood et al. 2009).

## Material and Methods

### *Experimental Animals*

Rainbow trout, *Oncorhynchus mykiss*, were obtained from Humber Springs Trout Farm in Orangeville and acclimated for at least 2 wk to 15° ± 0.5°C in flowing dechlorinated Hamilton tap water ($Na^+$ = 0.6, $Cl^-$ = 0.7, $K^+$ = 0.05, $Ca^{2+}$ = 1.0 mmol $L^{-1}$; pH = 8.0) under a 12-h light photoperiod. Fish were fed a commercial fish feed every 2 d until experiments when feeding was suspended 48 h before experimentation. Animals were cared for in accord with the principles of the Canadian Council on Animal Care, and protocols were approved by the McMaster Animal Care Committee. All protocols were designed to maximize the accuracy of branchial flux measurements over the critical exposure and to ensure that the external to internal specific activity ratios remained high for greatest accuracy in radioisotopic flux determinations while the water ammonia levels remained low. Therefore, different container volumes and experimental durations were used in different trials. A pilot experiment with juvenile trout demonstrated that the threshold for inhibitory effects of environmental hypoxia on branchial $Na^+$ influx lay between water $Po_2$ = 120 and 100 mmHg, so our experiments focused on this range and below.

### *Exposure Regimes*

*Unidirectional $Na^+$ Influxes, Effluxes, and Net Fluxes and Net Ammonia Fluxes in Response to Progressive (4 h) Hypoxia and Acute Normoxic Recovery.* Adult rainbow trout (395.4 ± 12.4 g, $n$ = 6) were transferred to separate, darkened, well-aerated acrylic flux boxes (4 L) with flow-through water supply (0.5 L $min^{-1}$) that were partially submerged in an external water bath to maintain temperature. After an overnight settling period, the experimental design consisted of a 3-h control normoxic period, a 4-h experimental hypoxic period, and a subsequent 3-h recovery normoxic period. Environmental hypoxia was induced by bubbling $N_2$ and air at a low rate in the individual tanks to bring the $Po_2$ of the holding water gradually down to a desired level of hypoxia over 4 h ($Po_2 \sim 110$ mmHg).

During the experiment, flux boxes were operated as closed systems at a volume of 2 L for the control normoxic period and at 2.25 L for the subsequent 4-h hypoxic exposure and 3-h normoxic recovery periods. Water was completely changed by flushing boxes (without air exposure of the fish) between the control normoxic period and the subsequent hypoxic exposure. Radioisotope ($^{22}Na$, 2.0 $\mu$Ci $box^{-1}$) was added immediately after the flushes at 0 h of the control normoxic period and before the hypoxic exposure. After an initial 10-min mixing period, a water sample (40 mL) was taken and subsequently at 1-h intervals until the end of the experiment for analysis of external [$Na^+$], total external ammonia ([Amm]), and $^{22}Na$ radioactivity (counts per minute [cpm]). Water $Po_2$ was monitored (1-mL samples) at the beginning of each 1-h flux. At the end of the experiment, the fish were anesthetized (neutralized MS-222, 0.075 g $L^{-1}$) and a blood sample taken by caudal puncture into a heparinized syringe. Plasma was separated by rapid centrifugation (10,000 *g* for 1 min) and frozen for analysis of internal $^{22}Na$ radioactivity (cpm) and internal [$Na^+$] levels. The fish were then immediately killed by an overdose of neutralized MS-222 (0.5 g $L^{-1}$).

*Unidirectional $Na^+$ Influxes, Effluxes, and Net Fluxes and Net $K^+$ and Ammonia Fluxes in Response to Prolonged Acute (8 h) Hypoxia.* Adult rainbow trout (188.1 ± 8.7 g, $n$ = 8) were transferred to the same flux boxes as used in experiment 1 and allowed to settle overnight. Experimental design consisted of a 3-h control normoxic period and a subsequent 8-h hypoxic exposure period. Hypoxia was induced by an $N_2$/air mixture that was empirically adjusted using a gas mixing pump (Wösthoff 301-af) to a desired level of hypoxia ($Po_2 \sim 80$ mmHg).

During the experiment, flux boxes were operated as closed systems at a volume of 2.5 L for the control normoxic period and at 3.5 L for the subsequent 8-h hypoxic exposure. Water was completely flushed and changed in the flux boxes between the control normoxic period and the subsequent hypoxic exposure. Radioisotope ($^{22}$Na, 2.0 $\mu$Ci box$^{-1}$) was added immediately after the flushes at 0 h of the control normoxic period and ($^{22}$Na, 4.0 $\mu$Ci box$^{-1}$) before the hypoxic exposure. The external radioisotope concentration was doubled at the beginning of hypoxia so as to raise the external specific activity sufficiently to minimize the need for backflux correction. After an initial 10-min mixing period, a water sample (30 mL) was taken and subsequently at 1-h intervals until the end of the experiment for analysis of external [$Na^+$], external [$K^+$], total external ammonia ([Amm]), and $^{22}$Na radioactivity (cpm). Water $Po_2$ was monitored (1-mL samples) at the beginning of each 1-h flux. At the end of the experiment, the fish were anesthetized (neutralized MS-222, 0.075 g L$^{-1}$) and a blood sample taken by caudal puncture into a heparinized syringe. Plasma was separated for analysis of internal $^{22}$Na radioactivity (cpm) and internal [$Na^+$] levels, and the fish were then killed as in experiment 2.

*The Effect of Acute Hypoxia (4 h) and Normoxic Recovery on Branchial $Na^+/K^+$-ATPase and $H^+$-ATPase Activities and Gill Morphology.* Adult rainbow trout ($n = 6$ per sampling point, 30 in total, mass 193.8 ± 6.1 g) were transferred to the same flux boxes as used in the previous experiments with flow-through water supply (0.5 L min$^{-1}$) and left overnight. The experimental design of this experiment 3 consisted of a control normoxic period, 4-h hypoxia exposure, and a subsequent 6-h normoxic recovery period. Hypoxia was induced by an $N_2$/air mixture that was empirically adjusted using a gas mixing pump (Wösthoff 301-af) to the desired level of hypoxia ($Po_2 \sim 80$ mmHg).

During the experiment, flux boxes were operated as closed systems at a volume of 3 L. Water was completely flushed and changed in the flux boxes (without air exposure of the fish) between the control normoxic period and the subsequent hypoxic exposure. Fish were rapidly killed with a lethal dose of anesthetic (0.5 g L$^{-1}$ neutralized MS-222) during normoxia, after 1 and 4 h of hypoxia, and after 1 and 6 h of normoxic recovery. Water $Po_2$ (1-mL samples) was also measured at each sampling time point. The second gill arch was excised and snap-frozen in liquid $N_2$ and stored at −80°C for later analysis for $Na^+/K^+$-ATPase and $H^+$-ATPase activities. The third gill arch was dissected out, quickly rinsed in water, and immediately fixed in cold Karnovsky's fixative. These samples were later transported to San Diego State University, California, for SEM.

### *Analytical Methods for Fluxes and Flux Calculations*

Water $Po_2$ was monitored by injecting a 1-mL sample into an $O_2$ electrode (Radiometer-Copenhagen, Denmark) thermostated to the experimental temperature and connected to a oxygen meter (A-M Systems polarographic amplifier, Kingston, Ontario). Water total ammonia (salicylate hypochlorite assay; Verdouw et al. 1978) was determined colorimetrically. Water total $Na^+$ and $K^+$ concentrations were measured using flame atomic absorption spectrophotometry (AAnalyst 800, Perkin Elmer). $^{22}$Na radioactivity was measured using a gamma counter (Minaxi Auto-Gamma 5000 Series, Canberra-Packard, Meriden, CT), where absolute counts were calculated from cpm values after background correction.

In experiments 1 and 2, $Na^+$ flux calculations were on the basis of equations presented by Kirschner (1970), Wood and Randall (1973*a*), and Wood (1992). Net $Na^+$ flux rates ($J_{net}^{Na}$) were calculated from the change in total $Na^+$ concentration in the water (factored by time, volume, and fish mass):

$$J_{net}^{Na} = \frac{([X_i] - [X_f]) \times V_{ext}}{W \times T}, \quad (1)$$

where $[X_i]$ and $[X_f]$ are total $Na^+$ concentrations ($\mu$mol L$^{-1}$) in the external water at the start and end of each 1-h flux period, $V_{ext}$ is the external water volume (L), $W$ is the weight of the fish (kg), and $T$ is the time (1 h). Net flux rates of ammonia ($J^{Amm}$) and $K^+$ ($J^K$) in all experiments were calculated as for $J_{net}^{Na}$.

$Na^+$ influx rates ($J_{influx}^{Na}$; by convention positive) were calculated from the mean external specific activity over each 1-h flux period and the disappearance of counts from the external water (factored by time, volume, and fish mass). Backflux correction (Maetz 1956; Kirschner 1970) was applied by the end of the experiment when internal specific activity reached about 10% of external specific activity. Therefore, influx was calculated as

$$J_{influx}^{Na} = \frac{([R_i] - [R_f]) \times V_{ext} - SA_{int}([X_i] - [X_f]) \times V_{ext}}{(SA_{ext} - SA_{int}) \times W \times T}, \quad (2)$$

where $[R_i]$ and $[R_f]$ represent initial and final $^{22}$Na radioactivity (cpm L$^{-1}$), $SA_{int}$ and $SA_{ext}$ are the mean internal and external specific activities (cpm $\mu$mol$^{-1}$) over the 1-h flux period, and the other symbols are as in equation (1). $SA_{int}$ at each time was estimated as described by Maetz (1956). In the calculation of $SA_{int}$, values of the internal distribution volume of $Na^+$ and the exchangeable internal pool of $Na^+$ were based on terminal plasma measurements. Unidirectional Na efflux rates ($J_{efflux}^{Na}$; by convention negative) were calculated by difference:

$$J_{efflux}^{Na} = J_{net}^{Na} - J_{influx}^{Na}. \quad (3)$$

### *Gill $Na^+/K^+$-ATPase and $H^+$-V-ATPase Enzyme Activities*

Gill $Na^+/K^+$-ATPase activity was measured on crude gill homogenates using the methods outlined by McCormick (1993), and gill $H^+$-ATPase activity was measured employing Lin and Randall's (1993) methodology with minor modifications. *N*-ethylmaleimide (NEM) was used as an $H^+$-ATPase inhibitor, and sodium azide was used to remove background activity of

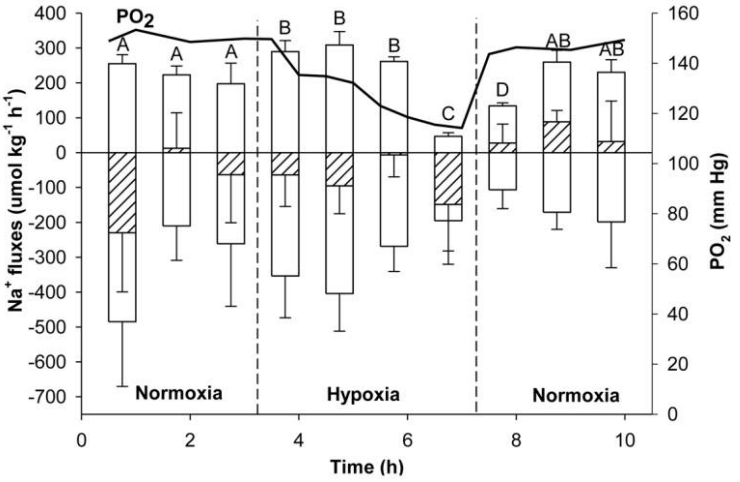


Figure 1. Mean $Na^+$ flux rates of adult rainbow trout ($N = 6$) to a progressive induction of hypoxia (down to ~110 mmHg) for 4 h followed by an acute restoration of normoxia in experiment 1: $Na^+$ unidirectional influx ($J^{Na}_{influx}$; *upward bars*), $Na^+$ efflux ($J^{Na}_{efflux}$; *downward bars*), $Na^+$ net flux rates ($J^{Na}_{net}$; *striped bars*), and water $O_2$ tension (*black line*). Values are expressed as means ± SEM. Means values of $J^{Na}_{influx}$ with the same letter are not significantly different from one another at $P \geq 0.05$. There are no significant differences among time periods in mean values of $J^{Na}_{efflux}$ and $J^{Na}_{net}$.

mitochondrial $H^+$-ATPases. An earlier comparison of bafilomycin versus *N*-ethylmaleimide showed that the two inhibitors produced identical results for $H^+$-ATPase activity in trout gills (Nawata et al. 2007). ATPase activities were normalized to total protein content (measured using Bradford Reagent [Sigma] and BSA standards) and expressed in $\mu$mol ADP $mg^{-1}$ protein $h^{-1}$.

*Morphological Analyses*

*SEM.* At San Diego State University, the middle part of each fixed gill arch (~4 mm long), bearing up to 12 filaments in both anterior and posterior rows, was used for SEM. Gill samples were rinsed in 0.1 M phosphate-buffered saline and post-fixed in 1% osmium tetroxide for 1 h. Then samples were dehydrated in ascending concentrations of ethanol from 30% to 100%, critical point dried with liquid $CO_2$, mounted on stubs, sputter coated with gold, and examined with a Hitachi S 2700 scanning electron microscope (Tokyo) at the accelerating voltage of 20 kV.

*Morphometry.* Gill parameters measured in control and experimental fish included density of MRCs (number of MRCs $mm^{-2}$) and surface area of individual MRCs. Quantification of MRC density was performed on randomly selected areas of the trailing edges of filaments located below the respiratory lamellae. SEM microphotographs (magnification × 2,000) of five randomly selected areas of filament epithelia of six fish (total number of measurements = 30) were analyzed, and the number of apical crypts of MRCs was counted. The surface area of 30 individual MRCs (five apical crypts for each of six fish examined in control and experimental conditions) was calculated on photographs at × 6,000 magnification according to the shape of their crypts, which varied from circular to oval, triangular, and roughly trapezoid.

*Statistical Analyses*

Data are reported as means ± SE (*N* is the number of fish), unless otherwise stated. Data were normally distributed; therefore, parametric statistics were used in all analyses. In experiments 1 and 2, where repeated measurements were made on the same fish, differences within experimental exposures (e.g., control vs. 1- and 4-h hypoxia) at different time periods were evaluated with a repeated-measures ANOVA followed by a post hoc test (Dunnett's multiple comparison test for paired data). In instances where ANOVA indicated significant variation but the post hoc test indicated no specific differences, a paired two-tailed Student's *t*-test was used to compare the overall mean value for the treatment period with that for the control period. To determine whether net fluxes were significantly positive or negative, a one-sample *t*-test was conducted, where mean net flux values were compared with 0. In experiment 3, statistical relationships were assessed by one-way ANOVA followed by Tukey's test for independent data. The level of significance was set at $P < 0.05$. All statistical tests were run using SigmaStat (ver. 3.1; Systat Software, San Jose, CA).

## Results

*Unidirectional $Na^+$ Influxes, Effluxes, and Net Fluxes and Net Ammonia Fluxes in Response to Progressive (4 h) Hypoxia and Normoxic Recovery*

The final target $Po_2$ was ~110 mmHg in this experiment. Progressive hypoxia (4 h) led to a significant change in mean $J^{Na}_{influx}$ starting at the onset of hypoxic exposure when $Po_2$ started to fall below 140 mmHg (Fig. 1). During the first 3 h of hypoxia exposure, $J^{Na}_{influx}$ was significantly elevated by about 21% compared with control normoxic rates. However, at 4 h of hypoxia, when $Po_2$ reached ~110 mmHg, there was a marked and sig-

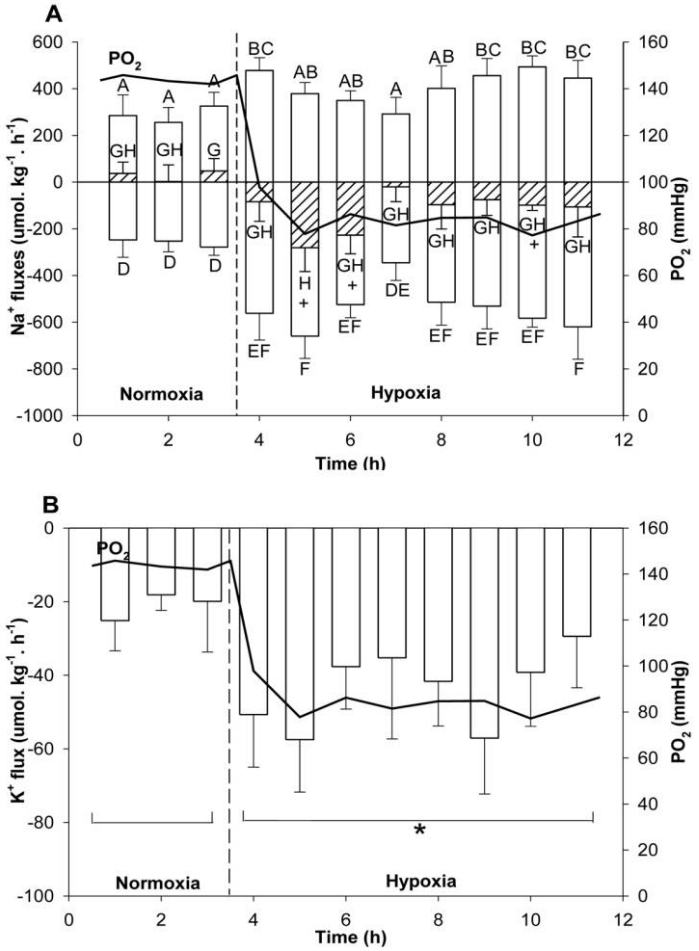


Figure 2. Mean $Na^+$ flux rates (*A*) and mean potassium ($K^+$) net flux rates (*B*) of rainbow trout ($N = 8$) subjected to acute induction of hypoxia (~80 mmHg) that was prolonged for 8 h subsequent to a 3-h normoxic control period in experiment 2: $Na^+$ unidirectional influx ($J^{Na}_{influx}$; *upward bars*), $Na^+$ efflux ($J^{Na}_{efflux}$; *downward bars*), $Na^+$ net flux rates ($J^{Na}_{net}$; *striped bars*), and water $O_2$ tension (*black line*). Values are expressed as means ± SEM. In *A*, means with same letter are not significantly different from one another, and plus signs denote a significant difference between mean $J^{Na}_{net}$ values and 0 (at a significance level of $P \leq 0.05$). In *B*, the asterisk denotes a significant difference between overall mean values of control and hypoxic exposures ($P \leq 0.05$).

nificant depression in $J^{Na}_{influx}$ to about 21% of normoxic values. $J^{Na}_{influx}$ remained significantly depressed during the first hour of normoxic recovery and was restored back to control rates during the second hour of normoxic recovery. There were no significant changes in $J^{Na}_{efflux}$ and $J^{Na}_{net}$ flux rates throughout the hypoxic exposure and subsequent normoxic recovery, and values of $J^{Na}_{net}$ were not significantly different from 0 (Fig. 1). Additionally, no significant changes were observed in mass-specific ammonia excretion rates, which averaged 129.7 ± 17.3 $\mu$mol $kg^{-1}$ $h^{-1}$ in the normoxic control period, 165.1 ± 19.5 $\mu$mol $kg^{-1}$ $h^{-1}$ in the hypoxic period, and 216.4 ± 44.4 $\mu$mol $kg^{-1}$ $h^{-1}$ in the normoxic recovery period ($N = 6$; data not shown).

### *Unidirectional $Na^+$ Influxes, Effluxes, and Net Fluxes and Net $K^+$ and Ammonia Fluxes in Response to Prolonged (8 h) Hypoxia*

Since we had observed a significant depression in $J^{Na}_{influx}$ rates at 4 h of hypoxic exposure (~110 mmHg; Fig. 1), this follow-up experiment examined sequential changes in flux rates in response to a more prolonged (8 h) and slightly more severe hypoxic (~80 mmHg) exposure (Fig. 2*A*, 2*B*). In this experiment, water $Po_2$ was acutely lowered over the first hour. In comparison to the 3-h control normoxic exposure, unidirectional $Na^+$ fluxes during 8 h of hypoxia displayed a triphasic response (Fig. 2*A*). $J^{Na}_{influx}$ was significantly elevated during the first hour of hypoxic exposure, similar to the response seen during the first hour in experiment 1 (Fig. 1). During the subsequent 3 h (2, 3, and 4 h of hypoxia), $J^{Na}_{influx}$ rates were reduced back to control levels (Fig. 2*A*). Thereafter, rates then started to gradually increase and remained significantly elevated by about 38% for the last 3 h of hypoxia (6, 7, and 8 h of hypoxia) compared with control rates. A similar triphasic trend was observed with $J^{Na}_{efflux}$ but with larger changes than in $J^{Na}_{influx}$. There were significant increases in $J^{Na}_{efflux}$ during early hypoxia, followed by correction and then increases again late in hypoxia (Fig. 2*A*). Negative $Na^+$ balance (i.e., $J^{Na}_{net}$ values significantly

below 0) was observed during the second, third, and seventh hour of hypoxic exposure in comparison to the zero $Na^+$ balance in the control normoxic period (Fig. 2*A*). After 2 h of hypoxic exposure, there was a significantly more negative $J_{net}^{Na}$ flux rate compared with the control normoxic period.

Net $K^+$ loss rates to the water approximately doubled in response to prolonged hypoxia, and overall there was a significant increase compared with normoxic control levels (Fig. 2*B*). Similar to experiment 1, mass-specific ammonia excretion rates showed no significant changes, averaging 166.9 ± 17.0 $\mu$mol $kg^{-1}$ $h^{-1}$ in the normoxic control period and 217.8 ± 13.3 $\mu$mol $kg^{-1}$ $h^{-1}$ during prolonged hypoxia ($N = 8$; data not shown).

### *The Effect of Acute Hypoxia (4 h) and Normoxic Recovery on Branchial $Na^+/K^+$-ATPase and $H^+$-ATPase Activities*

The hypoxia exposure protocol in this terminal sampling experiment essentially duplicated that of experiment 2 for the first 4 h of acute exposure to reduced $Po_2$ but was followed by 6 h of normoxic recovery. Branchial $Na^+/K^+$-ATPase activity did not change with acute hypoxia ($Po_2 \sim 80$ mmHg) or with normoxic restoration (Fig. 3).

Patterns in branchial $H^+$-ATPase activity were similar (Fig. 3). Gill $H^+$-ATPase activity did not change after 1 or 4 h of hypoxic exposure or after 1 h of normoxic recovery. However, $H^+$-ATPase activity was significantly depressed after 6 h of normoxic restoration to about 25% of the control activity.

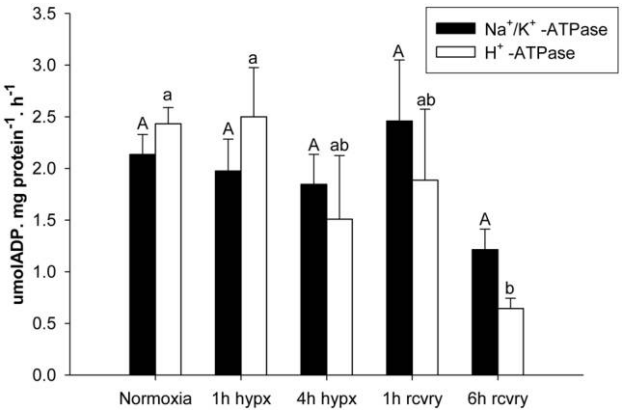


Figure 3. Gill $Na^+/K^+$-ATPase and $H^+$-ATPase activity changes in adult rainbow trout ($N = 8$ per sampling time) in response to acute induction of hypoxia (~80 mmHg) for 4 h followed by normoxic recovery in experiment 3. Values are expressed as means ± SEM. Means with the same letter of the same case are not significantly different from one another at $P \geq 0.05$.

### *The Effect of Acute Hypoxia (4 h) and Normoxic Recovery on Gill Morphology*

Gill morphology was studied in this same experiment. During normoxia, pavement cells (PVCs), the major component of the gill epithelium, exhibited a complex surface pattern composed of branched microridges (Fig. 4*A*). Numerous MRCs were distributed along the trailing edge of gill filaments, below respiratory lamellae (BRL) and in the interlamellar regions (ILRs; Fig. 4*A*). In normoxia, MRCs were grouped in clusters of three to five large cells, while beneath the lamellae, the MRCs were either solitary or gathered into clusters of two to four cells (Fig. 4*A*). Commonly, the apical crypts of the MRCs were flat and exhibited elongated straight microvilli that were raised above the level of the PVCs' surface (Fig. 5*A*, 5*B*). Some MRCs had slightly concave apical openings with short microvilli (Fig. 5*B*). The lamellar surface was formed by PVCs and exhibited few MRCs that were located only in the junctional regions between filament and lamellae (Fig. 4*A*).

After 1 h of hypoxia (~80 mmHg), the number of MRCs $mm^{-2}$ of gill filament epithelium was increased by 31% compared with MRC density during normoxia (Fig. 6*A*). MRCs in the ILRs were still organized into clusters of two to four or rarely five cells, while in BRL areas they were mostly solitary and rarely formed two-cell clusters (Fig. 5*B*). The surface area of individual MRCs and the percentage of the gill epithelium surface occupied by MRCs increased three- to fourfold compared with the same parameters in normoxic fish (Fig. 6*B*, 6*C*). MRC apical crypts became convex and displayed either short or stubby knoblike microvilli or an almost smooth surface with completely reduced microvilli (Fig. 5*C*, 5*D*). A limited number of MRCs demonstrated a novel carpetlike surface pattern composed of highly interdigitated microvilli that were not found in normoxic fish (Fig. 5*C*). Mucous cells were found to excrete huge globs of mucus at 1 h of hypoxia (Fig. 5*D*). After 4 h of hypoxia, the density of MRCs was reduced to control levels (Fig. 6*A*). MRC clusters disappeared, and instead solitary MRCs were present (Fig. 5*C*). Although the surface area of individual apical crypts and the percentage of surface area occupied by MRCs declined by almost 50% compared with 1-h hypoxia exposure, these characteristics remained significantly larger than those in normoxic conditions (Fig. 6*B*, 6*C*). MRC surfaces had either a flat carpetlike appearance or a convex surface with knoblike microvilli (Figs. 4*C*, 5*E*). Excessive mucus formed thin patches that covered the surfaces of epithelial cells (Fig. 5*F*). No changes were observed by SEM in the surface structure of the lamellar epithelium during exposure to hypoxia.

After return to normoxic water, there were morphological indications of recovery. After 6 h in normoxic water, MRC density was restored (Fig. 6*A*), and MRC clusters composed of two to three cells reappeared in ILRs and BLRs (Figs. 4*D*, 5*H*). However, the exposed surface area of individual apical crypts and the total surface area occupied by MRCs remained significantly elevated by about twofold compared with the same values in normoxic fish gills (Fig. 5*B*, 5*C*). Solitary MRCs showed a wide variety of surface patterns (Figs. 4*D*, 5*G*). Cells joined into clusters had either knoblike or more extended microvilli (Fig. 5*H*). Large, actively functioning mucous cells were also evident (Fig. 5*D*, 5*F*).

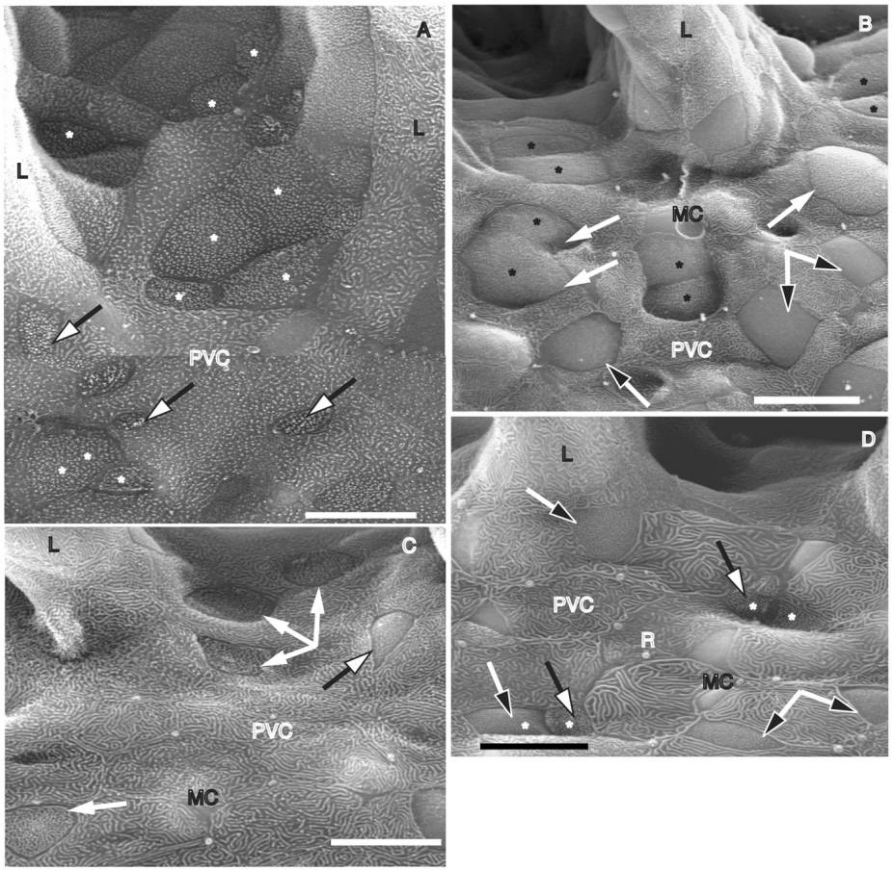


Figure 4. SEM photographs of surface structure and cellular composition of the epithelium covering the trailing edge of gill filaments of adult rainbow trout in normoxic water (*A*), exposure to experimental hypoxia (*B*, *C*), and after recovery in normoxic water (*D*) in experiment 3. *A*, Normoxia (control). Filamental epithelium covering interlamellar regions and areas below respiratory lamellae. Note clusters of three to five mitochondria-rich cells (MRCs) with apical surface ornamented with short microvilli in the interlamellar region (*asterisks*) and MRCs with long microvilli located below (*whitehead arrows*). *B*, 1-h hypoxic exposure. Note clusters of huge MRCs (*asterisks*) and large solitary MRCs with a convex apical surface with knoblike or completely reduced microvilli (*blackhead arrows*) and MRCs with a carpetlike surface composed of highly interdigitated microvilli (*white arrows*). *C*, 4-h hypoxic exposure. Lesser number of MRCs, no cell clusters. Solitary MRCs in the interlamellar area and below have either convex surface with knoblike microvilli (*blackhead arrows*) or flat carpetlike appearance (*white arrows*). *D*, 6-h normoxic recovery. Reappearance of clusters of MRCs (*asterisks*) with extended microvilli or knoblike microvilli (*whitehead arrows*). Solitary MRCs with convex surface covered by knoblike microvilli (*blackhead arrows*). *L*, lamella; *MC*, mucous cell; *PVC*, pavement cell; *R*, receptor. Scale bars = 10 $\mu$m.

## Discussion

### *Ionoregulatory Responses during Hypoxia in the Freshwater Rainbow Trout*

The focus of this study was on the ionoregulatory responses at the gills of the rainbow trout under hypoxia. We measured fluxes across the whole animal, assuming the gills to be the predominant site of exchange. While the kidney is known to contribute to ion and ammonia losses via dilute urine in freshwater fish, fluxes through this route are typically less than 10% of total losses (McDonald and Wood 1981; McDonald and Rogano 1986; Marshall and Grosell 2006). Overall, our results indicate that environmental hypoxia induces changes in gill ionoregulatory function in the freshwater adult rainbow trout, the direction and magnitude of which vary with both the extent and the duration of the hypoxia regime. The bidirectional nature of the ionoregulatory changes (i.e., both increases and decreases in ion fluxes, dependent on the extent and duration of hypoxia) suggests a more complex set of responses in this hypoxia-intolerant species compared with those seen in the hypoxia-tolerant Amazonian oscar (Wood et al. 2007, 2009). Moreover, unlike the situation in the oscar, some of the changes observed in trout do not appear to be adaptive.

### *Responses in $Na^+$ Efflux*

In our first hypothesis (see "Introduction"), we predicted that unidirectional $Na^+$ efflux rates to the water should increase under hypoxia. This hypothesis proved to be only partially confirmed. With progressive mild hypoxia down to 110 mmHg over 4 h in experiment 1, we did not see any significant changes in $J^{Na}_{efflux}$ (Fig. 1); however, $J^{Na}_{efflux}$ significantly increased in re-

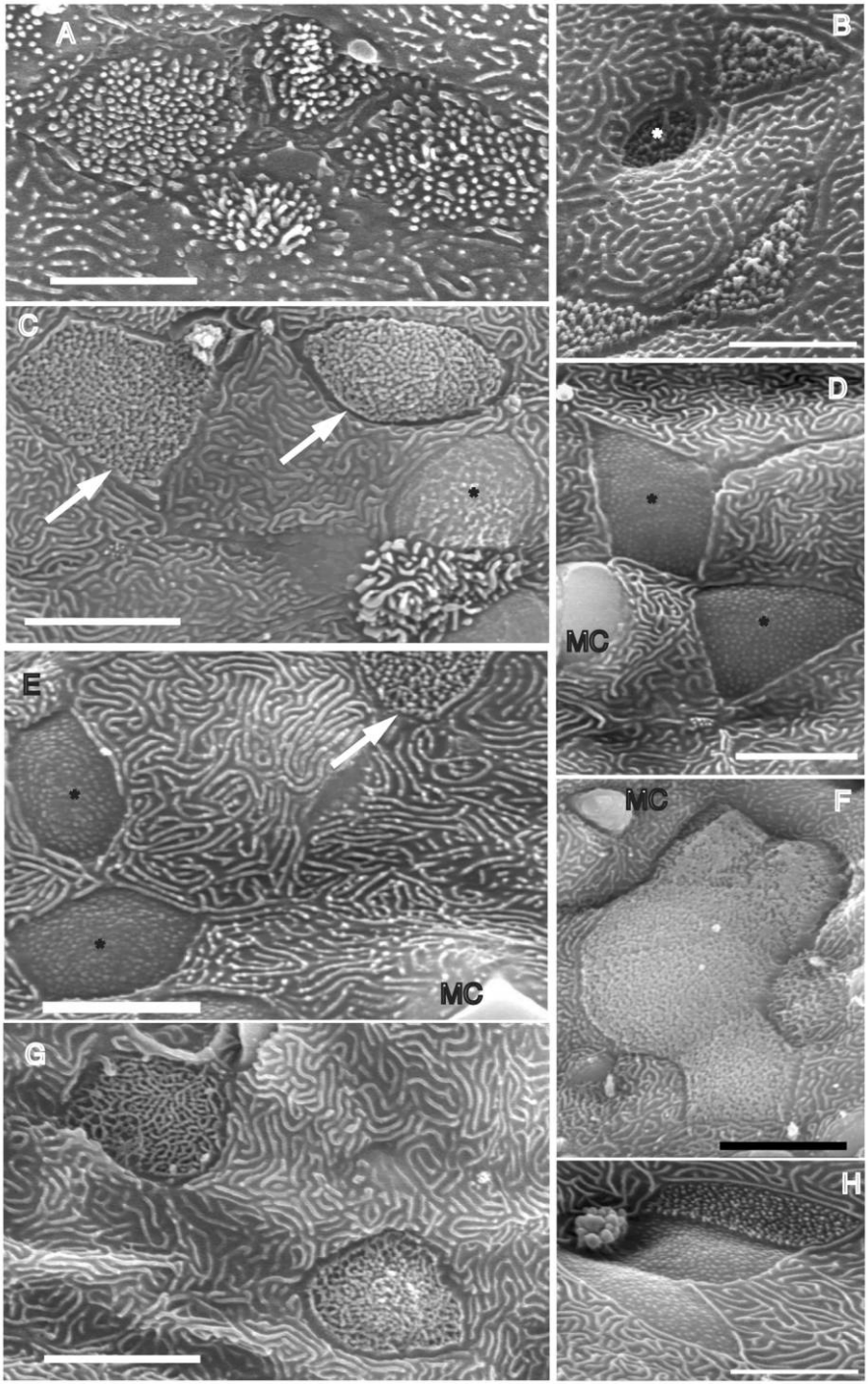


Figure 5. SEM photographs of surface structure of mitochondria-rich cells (MRCs) from the filamental epithelium of adult rainbow trout in normoxic water (*A*, *B*), hypoxia exposure (*C–F*), and normoxic recovery (*G*, *H*) in experiment 3. *A*, *B*, Normoxia, control. *A*, Cluster of four MRCs with slightly convex apical surface bearing long and straight microvilli, indicated by whitehead arrows in figure 4*A*. *B*, Clusters of two MRCs, one of which has a small concave apical crypt and short microvilli (*asterisk*). Apices of other cells are flat and bear straight microvilli. *C*, *D*, 1-h hypoxia exposure. MRCs with convex apices with knoblike microvilli (*asterisks*) are the most common in the epithelium. Some MRCs show novel carpetlike surface appearance (*white arrows*). Note glob of mucus released by mucous cells (MCs; *D*). *E*, *F*, 4-h hypoxia exposure. Surfaces of MRCs are convex and demonstrate either knoblike (*asterisks*) or carpetlike (*white arrows*) patterns. Mucus released from the MCs forms a thin film masking the surface of neighboring MRCs (*F*). *G*, *H*, 6-h normoxic recovery. MRCs with carpetlike apical surface (*G*) and cluster of three MRCs (*H*). Note knoblike microvilli in the middle and lower cells and longer microvilli in upper cells. Scale bars = 10 $\mu$m.

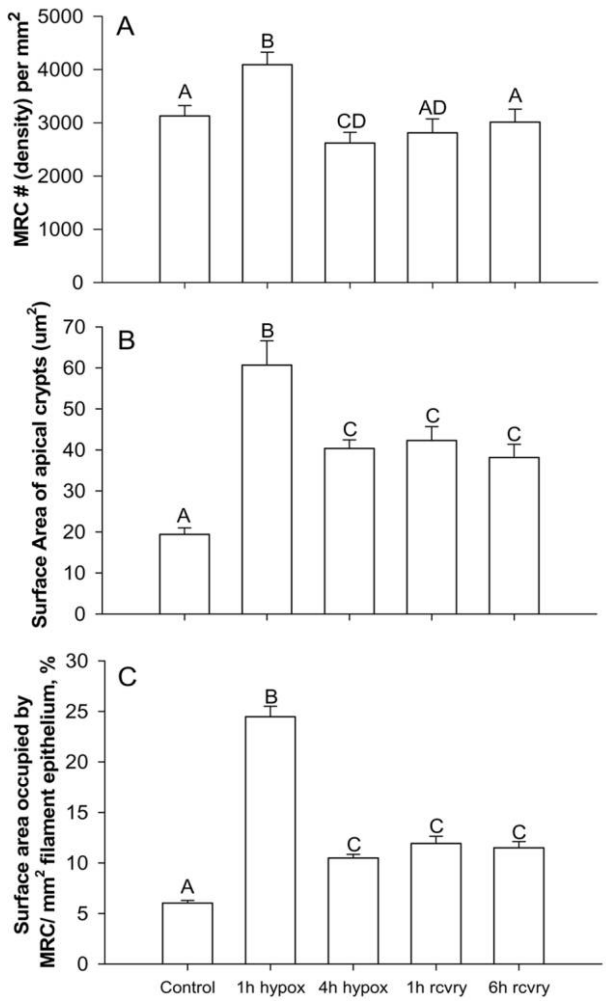


Figure 6. Quantitative morphometric analysis of changes in mitochondria-rich cells (MRCs) of the gill filamental epithelium in adult rainbow trout ($N = 8$ per sampling time) in response to acute induction of hypoxia (~80 mmHg) for 4 h followed by 6 h of normoxic recovery in experiment 3. *A*, MRC density in the filament epithelium. *B*, Surface area of apical crypts ($\mu m^2$). *C*, Surface area occupied by MRC $mm^{-2}$ in the filament epithelium (%). Values are expressed as means ± SEM. Means sharing the same letter are not significantly different from one another at $P \geq 0.05$.

sponse to a more prolonged (8 h) and slightly more severe hypoxic exposure (~80 mmHg) in experiment 2 (Fig. 2*A*). An initial elevation of $J^{Na}_{efflux}$ compared with normoxic levels during the first 3 h was reduced back to control levels by the fourth hour, followed by a second significant elevation of $J^{Na}_{efflux}$ in the last 4 h of hypoxia (Fig. 2*A*). $J^{Na}_{influx}$ followed a parallel triphasic pattern as $J^{Na}_{efflux}$. In part, these similar variations of $J^{Na}_{efflux}$ with $J^{Na}_{influx}$ may be explained by the phenomenon of exchange diffusion, a coupling of a portion of influx to efflux that results in no net transport; *Oncorhynchus mykiss* is a species that shows clear evidence of exchange diffusion in $Na^+$ transport (Randall et al. 1972; Wood and Randall 1973*b*). If the morphological area available for transport increases on either the blood or the water side, it is likely that the exchange diffusion fluxes will also increase, manifested as matching changes in $J^{Na}_{influx}$ and in $J^{Na}_{efflux}$.

However, the changes in $J^{Na}_{efflux}$ were not all due to exchange diffusion since they resulted in a changeover to significant net $Na^+$ loss (negative $J^{Na}_{net}$) in the second, third, and seventh hour of hypoxia (Fig. 2*A*). As mentioned in our initial hypothesis, this increased $J^{Na}_{efflux}$ may be explained by a rise in passive diffusion of electrolytes across the gill due to a change in blood flow pattern, which increases the area for gas transfer and ionic loss, similar to the situation during exercise (Randall et al. 1972; Wood and Randall 1973*a*, 1973*b*; Gonzalez and McDonald 1992, 1994; Postlethwaite and McDonald 1995). Closed lamellae are opened, and open lamellae are increasingly perfused (Booth 1979; Soivio and Tuurala 1981; Nilsson 1986; Sundin and Nilsson 1997). This, however, is very different from the response of the Amazonian oscar, which is able to downregulate $Na^+$ efflux so as to maintain ion balance during hypoxia (Wood et al. 2007, 2009), underlining an important difference between a hypoxia-tolerant and a hypoxia-intolerant teleost, with the latter exhibiting accelerated ion losses that are presumably maladaptive.

### *Responses in Ammonia Excretion*

In accord with our second hypothesis (see "Introduction") and in contrast with the Amazonian oscar (Wood et al. 2007), we observed no significant decreases in mass-specific ammonia excretion during either of the hypoxia regimes in the trout. In the oscar, the marked downregulation of ammonia excretion was attributed to both a downregulation in the ammonia production rate (van Waarde 1983) and a downregulation in gill permeability to ammonia during hypoxia (Wood et al. 2007, 2009). It is possible that these factors may have come into play in the trout, but the general response of trout is to exhibit increased ammonia production and efflux rates at times of stress, such as exercise (Wood 1988, 2001).

### *Responses in $Na^+$ Influx*

Branchial $Na^+$ influx was clearly very sensitive to even small changes in environmental oxygen levels. In experiment 1, our third hypothesis (see "Introduction") was partially supported. Progressive small reductions in $Po_2$ below 140 mmHg resulted in initial increases in $J^{Na}_{influx}$ followed by a significant depression after 4 h of exposure, once $Po_2$ reached 110 mmHg. This reduction in $J^{Na}_{influx}$ then persisted during the first hour of normoxic recovery (Fig. 1). Similarly, the Amazonian oscar exhibited a rapid and profound reduction of $Na^+$ uptake during 3 h of much more severe hypoxia (<20 mmHg), and this suppression of $Na^+$ influx was also seen during 1 h of normoxic recovery (Wood et al. 2007, 2009). While the fall in $J^{Na}_{influx}$ during hypoxia could be due to simple $O_2$ starvation (i.e., ATP limitation) of the ionocytes, it seems less likely that the continuation of the inhibition during normoxic recovery has the same explanation. A regulated phenomenon for conservation of met-

abolic energy at the level of transporters or channels, as proposed by Wood et al. (2007) for the oscar, could be involved.

In contrast to the oscar, the nature of the $J_{influx}^{Na}$ response in trout appears to depend on the severity and duration of the hypoxic exposure. With acute, slightly deeper hypoxia (80 mmHg) prolonged for 8 h in experiment 2, a triphasic response in $J_{influx}^{Na}$ was observed (Fig. 2*A*). As in the preceding experiment, there was an initial elevation of $J_{influx}^{Na}$ compared with normoxic levels during the first hour. During the subsequent 2–3 h, this uptake was reduced back to control levels, but there was no reduction in $J_{influx}^{Na}$ below control normoxic levels, in contrast to experiment 1. In turn, this was followed by a second significant elevation of $J_{influx}^{Na}$ in the last 3 h of hypoxia (Fig. 2*A*). This is contrary to our original hypothesis and previous observations in oscar (Wood et al. 2007, 2009).

We speculate that several competing factors may come into play here in the triphasic response, including changing blood flow patterns, exchange diffusion, $O_2$ limitations, acid-base status, and branchial ionocyte morphology. The initial increase in $J_{influx}^{Na}$ could be due to increased blood perfusion of the respiratory lamellae and/or the greatly increased MRC surface area at this time (Fig. 6). The subsequent fall in $J_{influx}^{Na}$ likely reflects the originally predicted $O_2$ starvation of transport processes, whereas the secondary increase could represent a combination of the stimulatory effects of acidosis and prolonged modest increases in MRC surface area. An increased lamellar perfusion as well as an overall increase in gill vascular resistance have been well documented during severe hypoxia ($Po_2 < 50$ mmHg) in trout (Holeton and Randall 1967*a*; Booth 1979; Soivio and Tuurala 1981; Sundin and Nilsson 1997), but it is not clear what happens during the more moderate hypoxia studied here. Catecholamine release is triggered with the onset of severe hypoxia in adult trout (Perry and Reid 1992; Reid and Perry 1994, 2003); the increase in circulating catecholamines serves to improve lamellar perfusion, thereby increasing the transfer factor of the gills for oxygen, which is an index of diffusing capacity (Holeton and Randall 1967*b*; Randall et al. 1972). The paradoxical increase in gill vascular resistance appears to be caused by a postlamellar cholinergic constriction, potentially diverting more blood flow to the central venous sinus, which underlies the filamental epithelium (Sundin and Nilsson 1997). There are more MRCs on the filamental epithelium than on the lamellae, but whether the blood-perfused "area" available for active ion uptake actually increases (which could explain increased $J_{influx}^{Na}$) is uncertain. Certainly, our morphological data indicate that the available area of filamental MRCs on the water side increases during moderate hypoxia (Fig. 4).

A study by Thomas et al. (1986), again using a more severe hypoxia (40 mmHg), showed a rapid, biphasic systemic acidosis over 20 min, probably representing catecholamine-driven extrusion of $H^+$ ions from red cells, followed by lactic acid mobilization. Given the more moderate $Po_2$ levels used here, which are well above the threshold for catecholamine release in trout (Perry and Reid 1992; Reid and Perry 2003), it is unlikely that the former occurred in our experiments. However, lactic acid production may well have taken place in the longer term exposures. This factor would also be expected to raise $J_{influx}^{Na}$ because of the well-known coupling of $Na^+$ influx to acidic equivalent excretion, as seen after exhaustive exercise in trout (Wood 1988).

### *Responses in Branchial $Na^+/K^+$-ATPase and $H^+$-ATPase Activities*

Note that the measurements of $Na^+/K^+$-ATPase and $H^+$-ATPase activities were made under optimal conditions in vitro, so we are measuring capacity and not the situation in vivo where ATP supply may be limiting. Contrary to our fourth hypothesis (see "Introduction"), we found no change in the activity of these pumps with 4 h of hypoxic (80 mmHg) exposure (Fig. 3). We expected a downregulation of these pump activities so as to conserve ATP in a situation where oxidative phosphorylation is slowed down by oxygen limitation during hypoxia (Boutilier and St-Pierre 2000). In contrast, the Amazonian oscar markedly downregulates branchial $Na^+/K^+$-ATPase activity after 3–4 h of severe hypoxia (Richards et al. 2007; Wood et al. 2007), so this appears to be another difference between the two species. However, many previous reviews indicate that absolute downregulation of ATP pumps occurs mainly when animals are subjected to anoxic conditions and/or face very severe lack of oxygen (Hochachka 1986; Boutilier and St-Pierre 2000; Hochachka and Lutz 2001), which was not the case in this study.

### *Responses in Net $K^+$ Loss Rates*

Interestingly, we saw net $K^+$ loss rates to the water approximately double with prolonged hypoxia, a significant increase compared with normoxic levels (Fig. 2*B*), suggesting cellular distress (Boutilier 2001) and providing support for our fifth hypothesis (see "Introduction"). This again contrasts with the Amazonian oscar, which loses less rather than more $K^+$ during severe hypoxia (Wood et al. 2009) and in which direct measurements have found no evidence of $O_2$ limitation in gill epithelial cells (Scott et al. 2008) or reductions in paracellular permeability (Wood et al. 2009). Cells are believed to lose intracellular $K^+$ when the $Na^+/K^+$-ATPase pump begins to fail with oxygen deprivation (Boutilier and St-Pierre 2000). This suggests that in vivo, ATP limitation may impact $Na^+/K^+$-ATPase activity during moderate hypoxia in trout, even though there was no change in enzyme capacity (Fig. 3). If the gill cells become depolarized during hypoxia, increased $K^+$ leak into the water would be expected (Boutilier and St-Pierre 2000; Boutilier 2001). Because $K^+$ concentrations inside cells are about 100-fold greater than those in blood plasma, Lauren and McDonald (1985) argued that $K^+$ loss rates at the gills of freshwater trout mainly reflect transcellular fluxes. Of course, it is possible that there is some paracellular flux of $K^+$, but it is likely small. Plasma $K^+$ levels are only 1.5% of plasma $Na^+$ levels in trout, whereas the net fluxes of $K^+$ and $Na^+$ to the water are similar, supporting the argument that $K^+$ efflux through the gills is largely transcellular.

*Hypoxia-Induced Changes in Gill Morphology*

In our final hypothesis (see "Introduction"), we predicted that any changes in the gill surface morphology of rainbow trout during hypoxia would be far less marked than in the oscar. To our surprise, there were in fact large changes in the numbers and surface areas of exposed MRCs on the filamental epithelium but in the opposite direction than seen in the oscar (i.e., both increased), and the effects persisted upon return to normoxia. In the Amazonian oscar, large reductions in both $J^{Na}_{efflux}$ and $J^{Na}_{influx}$ during hypoxia were accompanied by comparable reductions in the numbers and surface areas of exposed MRCs on the filamental epithelium, trends that were reversed during normoxic recovery (Wood et al. 2009). This disparity in response between the rainbow trout and oscar highlights the importance of adaptation to low environmental oxygen conditions by the latter.

In trout in normoxic water, MRCs were located in the outermost epithelial layer, occupying 6% of its surface, and appeared either as clusters or as solitary cells with a flat or slightly convex surface bearing long microvilli (Figs. 4*A*, 5*A*, 5*B*). It is known that in teleost fishes, some MRCs are located just beneath the leaflike PVCs that cover the vast majority of the gill epithelial surface (Wilson and Laurent 2002). The apices of these MRCs tended to be covered completely by PVCs and are usually not visible by SEM. Just 1 h of moderate hypoxic exposure (80 mmHg) caused immediate alterations in morphology of the filamental epithelium. The number of MRCs increased 1.3 times compared with control numbers, whereas their apical crypts expanded greatly such that the surface area (24%) occupied by MRCs was fourfold greater than in normoxic fish (Fig. 6). Our interpretation is that the previously "hidden" MRCs push out the PVCs that covered them, exposing the MRC apical openings to the environment. The reduced microvilli displayed by MRCs can be attributed to the stretching of this apical membrane (Figs. 4*B*, 5*C*, 5*D*). This initial distention may explain the initial increase observed in $J^{Na}_{influx}$ and $J^{Na}_{efflux}$ seen in experiment 2.

After 4 h of hypoxic exposure, rainbow trout adjusted their PVCs and MRCs so as to reduce the contact of the latter with the ambient water. Clusters of MRCs were dissociated, where solitary MRCs became less numerous and displayed a smaller surface area, but they still covered a twofold larger area in the filamental epithelium surface than in normoxic fish (Figs. 5*C*, 6). Concurrently, mucus was additionally deposited on the surface of filamental epithelial cells (Fig. 5*E*, 5*F*). This may serve to limit ion fluxes (note the concurrent decreases in $J^{Na}_{influx}$ and $J^{Na}_{efflux}$ at this time; Fig. 2*A*) without much negative impact on respiratory gas exchange, because the latter will occur through the respiratory lamellae. Reduction in the apical surface areas of MRCs, as well as in their number exposed to the environment, has been observed in the gills of various fish species as a response not only to hypoxia (Matey et al. 2008) but also to a number of other environmental stresses, such as high salinity (Sardella et al. 2004), low pH (Wendelaar Bonga et al. 1990), hypercapnia (Goss et al. 1994, 1998), and ion-poor water (Fernandes et al. 1998). Overproduction of mucus is considered as a generalized response of fish gills to a range of environmental stressors to which hypoxia can now be added (Matey et al. 2008). The return to normoxic water after 4 h of hypoxia caused a reappearance of MRC clusters, but the total surface area of exposed MRCs on the filament epithelium remained elevated (Fig. 6). The significance of this is unclear, but it may relate to the reductions in gill $H^+$-ATPase activity observed at this time (Fig. 3).

*Overview*

In conclusion, the ionoregulatory responses of rainbow trout to hypoxia are very different from those observed in the Amazonian oscar. Oscars respond to hypoxia by rapidly covering over their MRCs and reducing their gill ion and ammonia fluxes and $Na^+/K^+$-ATPase activities, thereby adapting to their natural environment, where hypoxia is a common occurrence (Almeida-Val et al. 2000; Wood et al. 2007, 2009). However, $Na^+$ flux responses of rainbow trout seem to depend on the length and severity of hypoxia, net $K^+$ and ammonia fluxes are not reduced, activities of gill $Na^+/K^+$-ATPase and $H^+$-ATPase remain unchanged, and increases in the apical exposure of MRCs occur. These differences in regulation may be attributed to the inherent physiology of the trout, a species that is poorly adapted to tolerate environmental hypoxia.

## Acknowledgments

This study was funded by a Natural Sciences and Engineering Research Council of Canada Discovery grant to C.M.W., who is supported by the Canada Research Chair Program. We thank Linda Daio, Andrea Morash, and John Fitzpatrick for their assistance during experimental setup.

## Literature Cited

Almeida-Val V.M.F., A.L. Val, W.P. Duncan, F.C.A. Souza, M.N. Paula-Silva, and S. Land. 2000. Scaling effects on hypoxia tolerance in the Amazon fish *Astronotus ocellatus* (Perciformes: Cichlidae): contribution of tissue enzyme levels. Comp Biochem Physiol B 125:219–226.

Booth J.H. 1979. The effect of oxygen supply, epinephrine, and acetylcholine on the distribution of blood flow in trout gills. J Exp Biol 83:31–39.

Boutilier R.G. 2001. Mechanisms of cell survival in hypoxia and hypothermia. J Exp Biol 204:3171–3181.

Boutilier R.G. and J. St-Pierre. 2000. Surviving hypoxia without really dying. Comp Biochem Physiol A 126:481–490.

Diaz R.J., J. Nestlerode, and M.L. Diaz. 2004. A global perspective on the effects of eutrophication and hypoxia on aquatic biota. Pp. 1–33 in G.L. Rupp and M.D. White, eds. Proceedings of the 7th International Symposium on Fish Physiology, Toxicology, and Water Quality, Tallinn, Estonia.

U.S. Environmental Protection Agency, Ecosystems Research Division, Athens, GA.

Evans D.H., P.M. Piermarini, and K.P. Choe. 2005. The multifunctional fish gill: dominant site of gas exchange, osmoregulation, acid-base regulation, and excretion of nitrogenous waste. Physiol Rev 85:97–177.

Fernandes M.N., S.A. Perna, and S.F. Moron. 1998. Chloride cell apical surface changes in gill epithelia of the armoured catfish *Hypostomus plecostomus* during exposure to distilled water. J Fish Biol 52:844–849.

Gonzalez R.J. and D.G. McDonald. 1992. The relationship between oxygen consumption and ion loss in a freshwater fish. J Exp Biol 163:317–332.

———. 1994. The relationship between oxygen uptake and ion loss in fish from diverse habitats. J Exp Biol 190:95–108.

Goss G.G., P. Laurent, and S.F. Perry. 1994. Gill morphology during hypercapnia in brown bullhead (*Ichthalurus nebulosus*): role of chloride cells and pavement cells in acid-base regulation. J Fish Biol 45:705–718.

Goss G.G., S.F. Perry, J.N. Fryer, and P. Laurent. 1998. Gill morphology and acid-base regulation in freshwater fishes. Comp Biochem Physiol A 119:107–115.

Hochachka P.W. 1986. Defense strategies against hypoxia and hypothermia. Science 231:234–241.

Hochachka P.W. and P.L. Lutz. 2001. Mechanism, origin, and evolution of anoxia tolerance in animals. Comp Biochem Physiol B 130:435–459.

Holeton G.F. and D.J. Randall. 1967*a*. Changes in blood pressure in the rainbow trout during hypoxia. J Exp Biol 46:297–305.

———. 1967*b*. The effect of hypoxia on the partial pressures of gases in the blood and water afferent and efferent to the gills of rainbow trout. J Exp Biol 46:317–327.

Kirschner L.B. 1970. The study of NaCl transport in aquatic animals. Am Zool 10:365–376.

Lauren D.J. and D.G. McDonald. 1985. Effects of copper on branchial ionoregulation in the rainbow trout, *Salmo gairdneri* Richardson. J Comp Physiol B 155:635–644.

Lin H. and D.J. Randall. 1993. $H^+$-ATPase activity in crude homogenates of fish gill tissue: inhibitor sensitivity and environmental and hormonal regulation. J Exp Biol 180:163–174.

Maetz J. 1956. Les échanges de sodium chez le poisson *Carassius auratus* L.: action d'un inhibiteur de l'anhydrase carbonique. J Physiol 48:1085–1099.

Marshall W.S. and M. Grosell. 2006. Ion transport and osmoregulation in fish. Pp. 177–230 in D. Evans, ed. The Physiology of Fishes. CRC, Boca Raton, FL.

Matey V., J.G. Richards, Y. Wang, C.M. Wood, J. Rogers, R. Davies, B.W. Murray, X.Q. Chen, J. Du, and C.J. Brauner. 2008. The effect of hypoxia on gill morphology and ionoregulatory status in the Lake Qinghai scaleless carp, *Gymnocypris przewalskii*. J Exp Biol 211:1063–1074.

McCormick S.D. 1993. Method for non-lethal gill biopsy and measurement of $Na^+$,$K^+$ ATPase activity. Can J Fish Aquat Sci 50:656–658.

McDonald D.G. and M.S. Rogano. 1986. Ion regulation by the rainbow trout, *Salmo gairdneri*, in ion poor water. Physiol Zool 59:318–331.

McDonald D.G. and C.M. Wood. 1981. Branchial and renal acid and ion fluxes in the rainbow trout, *Salmo gairdneri*, at low environmental pH. J Exp Biol 93:101–111.

Muusze B., J. Marcon, G. van den Thillart, and V.M.F. Almeida-Val. 1998. Hypoxia tolerance of Amazon fish: respirometry and energy metabolism of the cichlid *Astronotus ocellatus*. Comp Biochem Physiol A 120:151–156.

Nawata C.M., C.C.Y. Hung, T.K.N. Tsui, J.M. Wilson, P.A. Wright, and C.M. Wood. 2007. Ammonia excretion in rainbow trout (*Oncorhynchus mykiss*): evidence for Rh glycoprotein and $H^+$-ATPase involvement. Physiol Genomics 31: 463–474.

Nilsson S. 1986. Control of gill blood flow. Pp. 87–101 in S. Nilsson and S. Holmgren, eds. Fish Physiology: Recent Advances. Croom Helm, London.

Perry S.F. and S.D. Reid. 1992. Relationships between blood oxygen content and catecholamine levels during hypoxia in rainbow trout and American eel. Am J Physiol 263:R240–R249.

Postlethwaite E. and D.G. McDonald. 1995. Mechanisms of $Na^+$ and $Cl^-$ regulation in freshwater-adapted rainbow trout (*Oncorhynchus mykiss*) during exercise and stress. J Exp Biol 198:295–304.

Randall D.J., D. Baumgarten, and M. Malyusz. 1972. The relationship between gas and ion transfer across the gills of fishes. Comp Biochem Physiol A 41:629–637.

Randall D.J., G.F. Holeton, and E.D. Stevens. 1967. The exchange of oxygen and carbon dioxide across the gills of rainbow trout. J Exp Biol 46:339–348.

Reid S.G. and S.F. Perry. 1994. Storage and differential release of catecholamines in rainbow trout *Oncorhynchus mykiss* and American eel *Anguilla rostrata*. Physiol Zool 67:216–237.

———. 2003. Peripheral $O_2$ chemoreceptors mediate humoral catecholamine secretion from fish chromaffin cells. Am J Physiol 284:R990–R999.

Richards J.G., Y.S. Wang, C.J. Brauner, R.J. Gonzalez, M.L. Patrick, P.M. Schulte, V.M. Chippari-Gomes, V.M.F. Almeida-Val, and A.L. Val. 2007. Metabolic and ionoregulatory responses of the Amazonian cichlid, *Astronotus ocellatus*, to severe hypoxia. J Comp Physiol B 177:361–374.

Sardella B.A., V. Matey, J. Cooper, R.J. Gonzalez, and C.J. Brauner. 2004. Physiological, biochemical and morphological indicators of osmoregulatory stress in "California" Mozambique tilapia (*Oreochromis mossambicus* × *O. urolepis hornorum*) exposed to hypersaline water. J Exp Biol 207: 1399–1413.

Scott G.R., C.M. Wood, K.A. Sloman, F.I. Iftikar, G. De Boeck, V.M. Almeida-Val, and A.L. Val. 2008. Respiratory responses to progressive hypoxia in the Amazonian oscar, *Astronotus ocellatus*. Respir Physiol Neurobiol 162:109–116.

Sloman K.A., C.M. Wood, G.R. Scott, S. Wood, K. Kajimura, O.E. Johannsson, V.M.F. Almeida-Val, and A.L. Val. 2006. Tribute to R.G. Boutilier: the effect of size on the physiological and behavioural responses of oscar, *Astronotus ocellatus*, to hypoxia. J Exp Biol 209:1197–1205.

Soivio A. and H. Tuurala. 1981. Structural and circulatory responses to hypoxia in the secondary lamellae of *Salmo gairdneri* gills at two temperatures. J Comp Physiol B 135:37–43.

Sundin L. and G.E. Nilsson. 1997. Neurochemical mechanisms behind gill microcirculatory responses to hypoxia in trout: in vivo microscopy study. Am J Physiol 272:R576–R585.

Thomas S., B. Fievet, and R. Motais. 1986. Effect of deep hypoxia on acid-base balance in trout: role of ion transfer processes. Am J Physiol 250:R319–R327.

van Waarde A. 1983. Aerobic and anaerobic ammonia production by fish. Comp Biochem Physiol B 74:675–684.

Verdouw H., C.J.A. Van Echteld, and E.M.J. Dekkers. 1978. Ammonia determination based on indophenol formation with sodium salicylate. Water Res 12:399–402.

Wendelaar Bonga S.F., G. Flik, P.H.M. Balm, and J.C.A. van der Meij. 1990. The ultrastructure of chloride cells in the gills of the teleost *Oreochromis mossambicus* during exposure to acidified water. Cell Tissue Res 259:575–585.

Wilson J.M. and P. Laurent. 2002. Fish gill morphology: inside out. J Exp Zool 293:192–213.

Wood C.M. 1988. Acid-base and ionic exchanges at gills and kidney after exhaustive exercise in the rainbow trout. J Exp Biol 136:461–481.

———. 1992. Flux measurements as indices of $H^+$ and metal effects on freshwater fish. Aquat Toxicol 22:239–264.

———. 2001. The influence of feeding, exercise, and temperature on nitrogen metabolism and excretion. Pp. 201–238 in P.A. Anderson and P.A. Wright, eds. Fish Physiology. Academic Press, Orlando, FL.

Wood C.M., F.I. Iftikar, G.R. Scott , G. De Boeck, K.A. Sloman, V. Matey, F.X. Valdez Domingos, R.M. Duarte, V.M.F. Almeida-Val, and A.L. Val. 2009. Regulation of gill transcellular permeability and renal function during acute hypoxia in the Amazonian oscar (*Astronotus ocellatus*): new angles to the osmo-respiratory compromise. J Exp Biol 212:1949–1964.

Wood C.M., M. Kajimura, K.A. Sloman, G.R. Scott, P.J. Walsh, V.M.F. Almeida-Val, and A.L. Val. 2007. Rapid regulation of $Na^+$ fluxes and ammonia excretion in response to acute environmental hypoxia in the Amazonian oscar, *Astronotus ocellatus*. Am J Physiol 292:R2048–R2058.

Wood C.M. and D.J. Randall. 1973*a*. The influence of swimming activity on sodium balance in the rainbow trout (*Salmo gairdneri*). J Comp Physiol 82:207–233.

———. 1973*b*. Sodium balance in the rainbow trout (*Salmo gairdneri*) during extended exercise. J Comp Physiol 82:235–256.